Translational Oncology
www.transonc.com

Volume 12 Number 11 November 2019 pp. 1480–1487 1480

Impacts on Histological Features and ^{11}C-Methyl-L-methionine Uptake After "One-Shot" Administration with Bevacizumab Before Surgery in Newly Diagnosed Glioblastoma☆

Takaaki Beppu[1,*], Yuichi Sato[1], Noriyuki Yamada[2], Kazunori Terasaki[3], Toshiaki Sasaki[3], Tamotsu Sugai[2] and Kuniaki Ogasawara[1]

[1]Department of Neurosurgery, Iwate Medical University, Japan; [2]Department of Clinical Pathology, Iwate Medical University, Japan; [3]Cyclotron Research Center, Iwate Medical University, Japan

Abstract

BACKGROUND: Bevacizumab (BEV), an antiangiogenic agent, induces dramatic normalization of the tumor vasculature in glioblastoma. This study aimed to clarify how one-time administration of BEV changes histological features in glioblastoma and how histological changes affect the uptake of ^{11}C-methyl-L-methionine (^{11}C-met) as an amino-acid tracer. *MATERIALS AND METHODS:* Subjects were 18 patients with newly diagnosed glioblastoma who were assigned to two groups: BEV group, single intravenous administration of BEV before surgical tumor removal; and control group, surgical tumor removal alone. After surgery, we compared the densities of tumor cells and microvessels, and microvascular structures including vascular pericytes and L-type amino acid transporter-1 (LAT1) between the BEV and control groups. Correlations between ^{11}C-met uptake on positron emission tomography before surgery, microvascular density, and LAT1 expression were assessed in each group. *RESULTS:* BEV induced significant reductions in microvascular density, while tumor cell density and proliferation were retained in the BEV group. Percentages of vessels with pericytes and vascular endothelium with LAT1 expression were lower in the BEV group than in controls. Uptake of ^{11}C-met correlated significantly with microvascular density in the BEV group but not with LAT1expression. *CONCLUSIONS:* The present study showed that even one course of BEV administration induced reductions in microvessels, vascular pericytes, and LAT1 expression in glioblastomas. One course of BEV therapy also reduced ^{11}C-met uptake, which might have been largely attributed to reductions in microvessels rather than reductions in LAT1 expression.

Translational Oncology (2019) 12, 1480–1487

Introduction

Bevacizumab (BEV), a humanized anti—vascular endothelial growth factor (VEGF) antibody, has been applied to the treatment of glioblastoma, which is an obstinately malignant brain tumor with extensive vascularization [1]. In Japan, use of BEV has been allowed for recurrent and newly diagnosed glioblastoma since 2016. BEV contributes to restoration of the disrupted blood-brain barrier (BBB), leading to reduction of peritumoral edema [2]. Consequently, we can use BEV prior to surgical removal of the tumor in the initial treatment of glioblastoma, with the expectation of improving performance status in patients before surgery. Given that the speed of glioblastoma growth is still high even if BEV use is initiated, BEV treatment before the initial surgery may be reasonably limited to only a single course. In that situation, how BEV histologically affects glioblastoma tissue is

Address all correspondence to: Takaaki Beppu, M.D., Ph.D., Department of Neurosurgery, Iwate Medical University, 19-1 Uchimaru, Morioka, 020-8505, Japan.
E-mail: tbeppu@iwate-med.ac.jp
☆ Declarations of interest: none
Received 7 April 2019; Revised 1 August 2019; Accepted 2 August 2019

1936-5233/19
https://doi.org/10.1016/j.tranon.2019.08.002

crucial for pathological diagnosis and also assessments from preoperative neuroimaging, including positron emission tomography (PET).

Some retrospective studies have documented the histological impact of BEV on glioblastoma *in vivo* [3–5]. However, subjects in those reports comprised patients treated with several courses of BEV, and many had even already undergone surgery and/or radiation therapy before BEV initiation. We aimed to clarify histological changes after one course of BEV in patients with newly diagnosed glioblastoma. In addition to assessing densities of tumor cells and microvessels, we assessed the status of vascular pericytes and vascular endothelium with L-type amino acid transporter-1 (LAT1) expression. Neovascularization in glioblastoma has been considered to be caused by proliferation of vascular pericytes rather than of endothelial cells [6]. LAT1 is a sodium-independent neutral amino acid transporter and plays a role as a transporter of amino-acid metabolic tracers in PET. Furthermore, this study assessed relationships between the uptake of ^{11}C-methyl-L-methionine (^{11}C-met) as an amino-acid tracer on PET, vascular density, and LAT1 expression.

Materials and Methods

Patients

The present study was performed in accordance with the precepts established by the Declaration of Helsinki. All study protocols were approved by the ethics committee at our institute (No. H22-96). Subjects met the following entry criteria for the study: admission to our institute to receive initial treatment for a brain tumor located in the cerebral white matter; age $\geq$ 20 years; no history of treatment for brain diseases; need for preoperative treatment with BEV to maintain or rapidly improve neurological deficits until surgical tumor removal; performance of ^{11}C-met-PET immediately before surgery; diagnosis of glioblastoma based on histological findings; and voluntary provision of written informed consent to participate. Exclusion criteria included diabetes mellitus, active gastrointestinal ulcer, or inadequate hematological reserve for administration of BEV. Nine patients admitted between January 2016 and July 2018 were enrolled in this study as the BEV group (six men, three women; median age, 64 years; range, 46-72 years). We also randomly selected another nine patients who met the criteria described above other than preoperative BEV therapy as a control group (five men, four women; median age, 64 years; range, 41-72 years). The tumor was located in the frontal lobe in four patients, the temporal lobe in one patient, the parietal lobe in three patients, and the occipital lobe in one patient in the BEV group, and the frontal lobe in two patients, the temporal lobe in three patients, and the parietal lobe in four patients in the control group.

Preoperative Procedures

Patients in the BEV group were intravenously administered BEV at a dose of 10 mg/kg once only. The day of BEV administration was defined as day 0. Physiological observations including Karnofsky performance scale (KPS) and blood examinations were performed between BEV treatment and surgical removal to check for the presence of adverse events due to BEV. Administration of corticosteroid after BEV initiation was prohibited, whereas patients in the control group received corticosteroid if necessary. Conventional magnetic resonance imaging (MRI) including fluid-attenuated inversion recovery (FLAIR) and gadolinium enhanced T1-weighted imaging (Gd-T1WI) were performed on two occasions: within 3 days before BEV therapy for patients in the BEV group and within 3 days before surgery for all patients in both groups. Maximum tumor diameter was measured for all patients on Gd-T1WI before surgery. MRI was performed using a 3.0-T MRI system (Discovery MR750; GE Healthcare Japan, Tokyo, Japan).

All patients from both groups received ^{11}C-met-PET within 3 days before surgery. Four of nine patients in the BEV group underwent ^{11}C-met-PET, again within 3 days before BEV administration. Synthesizing tracer and scanning conditions have been provided in a previous report [7,8]. At 20 minutes after intravenous injection of methionine with a dose of 317-346 MBq (mean, 6.5 MBq/kg), ^{11}C-met-PET was scanned using a PET/computed tomography system (SET3000 GCT/M; Shimadzu, Kyoto, Japan). Maximum standardized uptake value (SUVmax) was automatically determined for all regions of interest as areas of 6 mm in diameter on the area of highest ^{11}C-met accumulation within the tumor, and on three regions in apparently normal cerebral white matter in the contralateral hemisphere, as previously reported [7]. Mean value of the three regions was calculated for SUVmax in normal tissue. The ratio of SUVmax in tumor to that in normal tissue ($SUV_{T/N}$) was calculated for each scan. All procedures for PET were performed by two investigators (T.S., K.T.) who were blinded to all clinical data.

Tumor Removal

For patients in the BEV group, tumor removal was performed after an interval of 3 weeks from BEV administration using standard neurosurgical techniques with a surgical image-guided navigation system (CURVE surgical system; Brainlab, Munich, Germany). During operations, tumors of all 18 patients were resected under visualization of the tumor as pink-colored tissue using 5-aminolevulinic acid (5-ALA) administered orally at 20 mg/kg body weight. Based on combined images of MRI with ^{11}C-met-PET on a surgical navigation system, we rigorously obtained tumor tissue samples from those regions showing the highest accumulation of ^{11}C-met. All treatment management was conducted by three investigators (T.B., Y.S., and K.O.). After tumor removal, adjuvant and concomitant therapies comprising radiation therapy combined with temozolomide were implemented for seven patients in the BEV group and six patients in the control group. The remaining two patients in the BEV group and three patients in the control group received BEV administration every 2 weeks in addition to the adjuvant/concomitant therapy described above. The decision on whether to add BEV was made at the discretion of the treating physicians. Progression-free survival (PFS) was defined as the number of days between date of operation and recognition of tumor recurrence on MRI and was evaluated in each patient.

Histopathological Procedures

Tumor specimens were fixed overnight in 10% formalin and then embedded in paraffin, and serial sections of 3-μm thickness were collected onto 3-aminopropyltriethoxysilane-coated glass slides for hematoxylin and eosin (HE) staining and immunohistochemical staining. Immunohistochemical staining was performed for isocitrate dehydrogenase-1 (IDH-1), VEGF-A (VEGFA), Ki-67, CD34, and α-smooth muscle antigen (α-SMA) as a marker of pericytes, and LAT1 on dewaxed sections pretreated with immersion for 20 minutes at 97 °C in sodium citrate buffer at pH 6-9 for antigen retrieval. The primary antibodies and incubation conditions were as follows: IDH-1 (1:80, monoclonal mouse anti-IDH-1 R132H antibody, clone, H09;

Dianova, Hamburg, Germany); VEGFA (0.8 μg/ml, rabbit polyclonal anti-human VEGFA antibody, #ab46154; Abcam, Cambridge, UK); Ki-67 (undiluted FLEX monoclonal mouse anti-human Ki-67 antibody, clone, MIB-1; Dako Japan, Tokyo, Japan); CD34 (undiluted FLEX monoclonal mouse anti-human CD34 Class II, clone, QBEnd 10; Dako Japan); α-SMA (undiluted FLEX monoclonal mouse anti-human αSMA, clone, 1A4; Dako Japan); and LAT1 (2 μg/ml, rabbit monoclonal anti-human SLC7A5 antibody, # ab208776; Abcam) for 30 minutes at room temperature. Staining using the secondary antibody was then conducted using a Dako REAL detection system (Dako REAL EnVision Detection System, #K5007; Dako Japan). After incubation procedures, preparations were immersed in diaminobenzidine/H_2O_2 solution for colored visualization of the reaction product. Finally, preparations were counterstained with hematoxylin. All histopathological procedures were performed by two investigators (N. Y., T. S).

Assessments and Analyses

All statistical data analyses were conducted using PASW Statistics version 18 software (SPSS Japan, Tokyo, Japan). Values of $P < .05$ were considered significant in all statistical analyses. KPS before BEV initiation was compared to that before surgery using the Wilcoxon signed-ranks test. Tumor location and maximum tumor diameter before surgery were compared between the BEV group and the control group using the χ^2 test for independence and the Mann-Whitney *U* test, respectively. PFS was compared between the BEV and control groups using the log-rank test.

Between findings of MRI before BEV therapy and before surgery, therapeutic response was assessed according to the current criteria of the Response Assessment in Neuro-oncology (RANO) [9,10]. Mean $SUV_{T/N}$ before surgery was compared between the nine patients in the BEV group and the nine patients in the control group using the Mann-Whitney *U* test. In the four patients in the BEV group who underwent consecutive PET, mean $SUV_{T/N}$ was compared between before BEV administration and before surgery using the Wilcoxon signed-ranks test. For those patients, the rate of change in $SUV_{T/N}$ was calculated using the following formula: ($SUV_{T/N}$ from later PET − $SUV_{T/N}$ from earlier PET) / $SUV_{T/N}$ from the earlier PET (%).

On HE-stained preparations, we examined the existence of the glomeruloid appearance and pseudopalisading necrosis. When either of these features was confirmed, we diagnosed the tissue sample as representing glioblastoma. When most tumor cells showed the presence or absence of IDH-1 antigen, we identified the tumor as IDH-mutant type or IDH-wild type, respectively. For assessment of VEGFA, the percentage of VEGFA-positive cells in 1000 cells was measured in each patient. Tumor cell density and vascular density were identified as the mean number of tumor cells excluding vessel cells and blood cells on HE preparations in 10 fields of a square measuring 250 μm per side, and the mean number of CD34-positive vessels on CD34-stained preparations in 10 fields of a square measuring 500 μm per side, respectively. Percentages of Ki-67−positive cells among 1000 cells were measured. Since α-SMA is supposedly expressed not only in vascular pericytes but also in endothelial cells [11], cells staining positively for α-SMA but negatively for CD34 (α-SMA+/CD34−) around vessels were identified as vascular pericytes, according to a previous report [3]. We measured the percentage of vessels accompanied by vascular pericytes among the total number of vessels staining positively for CD34 in 10 fields from a square measuring 500 μm per side for each patient. Expression of LAT1 was assessed as the percentage of LAT1-positive vessels among all CD34-positive vessels in 10 fields of a square measuring 500 μm per side. Finally, we compared values of VEGFA, cell density, vascular density, Ki-67, vessels accompanying with pericytes, and LAT1-positive vessels between the BEV and control groups using the Mann-Whitney *U* test.

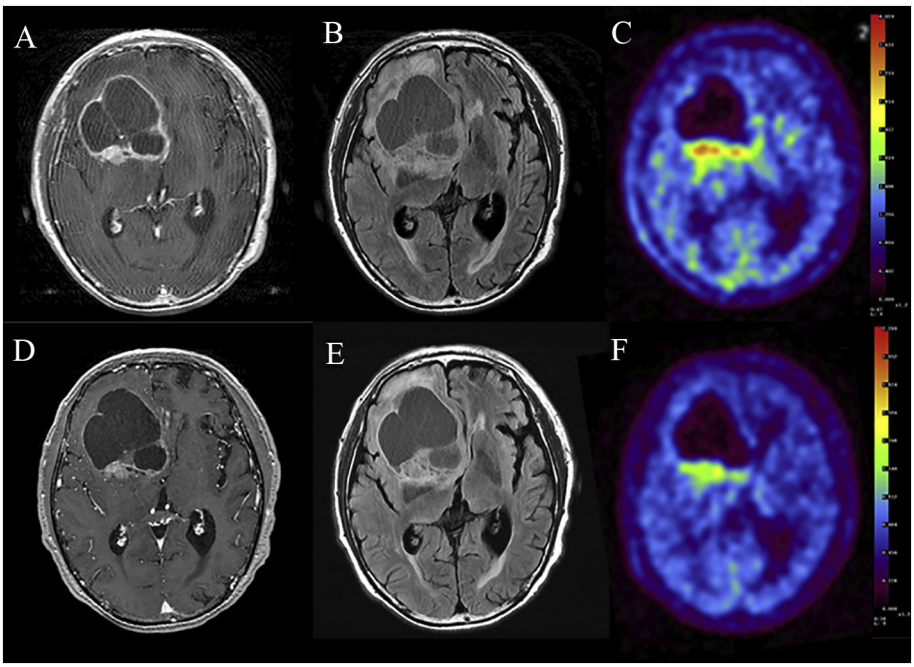

Figure 1. Representative results of Gd-T1WI (A, D), FLAIR (B, E), and ^{11}C-met-PET (C, F) before (upper row) and after BEV therapy (lower row) for case 3 in the BEV group. Therapeutic response on MRI remained as stable disease, whereas ^{11}C-met uptake was markedly reduced on PET after BEV therapy.

To verify relationships between ^{11}C-met uptake, vascular density, and LAT1 expression, we assessed correlations between $SUV_{T/N}$ before surgery and means of number of CD34-positive vessels and between $SUV_{T/N}$ before surgery and percentages of LAT1-positive vessels in each BEV and control group using Spearman's correlation coefficient from rank testing.

Results

Clinical Findings in the BEV Group

In patients from the BEV group, no clear adverse events were seen from physiological examinations and no blood examinations were performed before the operation. MRI after BEV therapy showed partial response in two patients and stable disease in seven patients according to RANO. Contrast enhancement within the tumor on Gd-T1WI after BEV therapy was alleviated but did not entirely disappear in all nine patients (Figure 1). KPS was increased in five patients and sustained in four patients. Median KPS before and after BEV therapy was 60% and 70%, respectively. KPS was significantly higher after BEV than before BEV ($P = .049$). $SUV_{T/N}$ before surgery was significantly lower for the BEV group (2.17 ± 0.70) than for the control group (2.77 ± 0.58, $P = .04$). In the four patients who underwent consecutive PET in the BEV group, BEV showed a tendency to reduce $SUV_{T/N}$ (before, 2.69 ± 1.02; after, 2.28 ± 0.77), although the difference was not significant ($P = .07$). The rate of change in $SUV_{T/N}$ for those four patients ranged from -6.2% to -19.4% (mean, $-14.4\% \pm 6.0\%$). Mean $SUV_{T/N}$ before BEV therapy in these four patients did not significantly differ from that before surgery for the nine patients in the control group ($P = .44$). (See Table 1.)

Location and maximum diameter of tumor in the BEV group showed no significant differences from those in the control group (location, $P = .29$; diameter, 54.0 ± 15.0 mm in the BEV group, 51.8 ± 8.5 mm, $P = .33$). In the BEV group, surgery was performed within the third week for eight patients and in the fourth week for one patient after BEV (range, 21-30 days; median, 25 days). During surgery in the BEV group, we felt that hemostasis for bleeding within the tumor was easier to achieve than usual. Tumor showed pink coloration due to 5-ALA in all tumors in the BEV group. After sampling tumor tissue corresponding to the regions of highest ^{11}C-met uptake, tumors were totally removed in all patients. After surgery, no clear complications such as intracranial hemorrhage or problems including the wound healing were seen in the BEV group. Removal of staples for skin sutures was performed within the second week after surgery. The follow-up period for the final patient latest recruited to this study was 8 months. Five patients in the BEV group and seven patients in the control group developed tumor recurrence. PFS showed no significant difference between the BEV group (median PFS, 216 days) and the control group (median PFS, 333 days; $P = .96$).

Histopathological Findings

On HE preparations, a few glomeruloid structures were seen in five patients in the BEV group, whereas tumors of all control patients showed frequent glomeruloid structures in preparations. Since pseudopalisading necrotic lesions were seen in all patients in both groups, all tumors in the BEV group were consequently diagnosed as glioblastoma. In the BEV group, however, layers of tumor cells surrounding necrotic regions tended to be thinner than usual (Figure 2). Immunohistochemical staining for IDH-1 showed negative results, suggesting IDH-wild type in all tumors in both groups.

Strongly positive staining for VEGFA was seen in the nuclei of tumor cells in all patients, but positive findings were significantly less frequent in the BEV group ($5.8\% \pm 8.0\%$) than in the control group ($21.5\% \pm 11.2\%$; $P < .01$) (Figure 3, *B*, *F*). Tumor cell density, Ki-67 positivity, and microvessel density (density of CD34-stained vessels) appeared lower in the BEV group than in controls. However, cell density and Ki-67 positivity did not show significant differences between the BEV group (cell density, 259 ± 101 cells; Ki-67, $23.2\% \pm 13.6\%$) and the control group (cell density, 345 ± 82 cells; Ki-67, $36.9\% \pm 29.7\%$; $P = .07$ for cell density; $P = .12$ for Ki-67). Mean number of CD34-positive vessels was significantly lower in the BEV group (18.9 ± 8.8 vessels) than in controls (38.8 ± 5.6 vessels; $P < .01$). CD34 was stained in thin layers representing the

Table 1. All Data from ^{11}C-met-PET and Immunohistochemistry

No.	$SUV_{T/N}$ Before BEV	$SUV_{T/N}$ Before Surgery	VEGFA (%)	Cell Density /250 μm^2	Ki-67 (%)	Microvessel Density (CD34) /500 μm^2	Vessels with Pericytes (%)	Vessels with LAT1 (%)
BEV group								
1	-	1.86	3.5	392	38.6	17.5	41.4	72.0
2	2.36	1.93	0.0	209	14.5	25.8	1.9	67.1
3	2.41	2.26	26.5	381	20.5	18.2	28.8	47.0
4	-	1.64	4.2	226	5.3	15.4	68.8	16.2
5	1.82	1.57	1.6	322	10.0	8.6	55.8	39.5
6	-	1.49	7.6	88	11.6	9.3	22.2	44.1
7	-	3.28	2.6	184	32.8	24.5	6.8	68.2
8	4.17	3.36	2.5	206	39.1	36.3	5.0	55.1
9	-	2.15	3.5	324	36.8	14.6	15.1	78.8
Control								
1	-	3.48	34.6	217	22.2	44.7	87.7	85.7
2	-	3.69	15.6	444	84.0	27.7	52.7	77.6
3	-	2.87	19.6	323	25.8	43.2	93.1	84.5
4	-	2.48	11.5	445	41.0	39.3	89.6	102.0
5	-	1.88	40.4	357	16.6	36.5	84.4	76.4
6	-	3.14	4.5	334	35.6	45.8	95.0	82.5
7	-	2.64	27.6	434	43.5	35.4	89.0	81.6
8	-	2.52	18.4	287	35.1	36.3	79.6	84.8
9	-	2.26	21.5	268	28.6	40.1	79.3	51.4

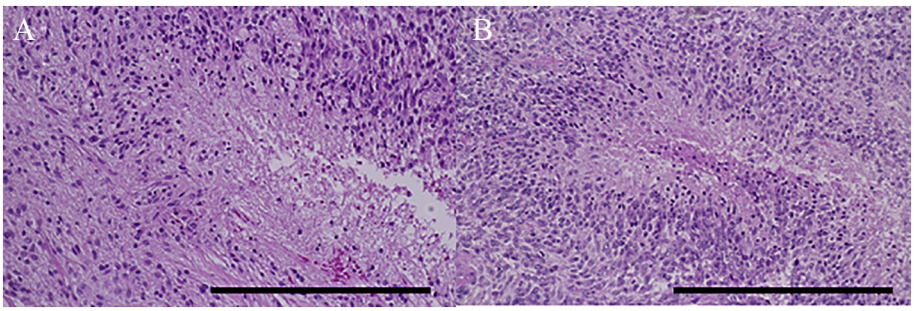

Figure 2. Necrotic lesions of case 4 in the BEV group (A) and case 16 in the control group (B). Necrotic lesions in the control group show a typical feature of "pseudopalisading," whereas accumulation of tumor cells surrounding necrotic regions in the BEV group is thinner. Bar = 250 μm.

endothelium of microvessels in tumors of both groups. Staining for α-SMA was seen in not only vascular endothelial layers but also cells surrounding vascular endothelium, which were identified as vascular pericytes in all cases. Vascular pericytes were accumulated much more thickly around the endothelium in the control group than in the BEV group (Figure 3, *C*, *D*, *G*, *H*). The mean percentage of vessels with pericytes was significantly lower in the BEV group (27.3% ± 23.6%) than in controls (83.4% ± 12.7%; $P < .01$). LAT1 was detected in the endothelial layer of microvessels in all tumors of both groups. Mean percentage of vessels with LAT1 expression was significantly lower in the BEV group (54.2% ± 19.7%) than in controls (80.7% ± 13.2%, $P < .01$; Figure 4).

CD34-positive vascular density correlated significantly with $SUV_{T/N}$ from PET before surgery in the BEV group (rs = 0.80, $P < .05$), whereas no such correlation was found in controls (rs = 0.10, $P = .78$, Figure 5, *A*, *B*). The percentage of vessels with LAT1 did not correlate significantly with $SUV_{T/N}$ from PET before surgery in either the BEV or control group (BEV, rs = 0.5, $P = .16$; control, rs< 0.1, $P = .81$; Figure 5, *C*, *D*). In the BEV group, however, tumors showing higher ^{11}C-met-uptake tended to contain many more microvessels showing LAT1 expression.

Discussion

Performance status before surgery is one of the prognostic factors in the treatment of glioblastoma [12]. We have taken advantage of BEV before surgery for patients with glioblastoma in expectation of effects such as dramatic alleviation of peritumoral vasogenic edema. This study showed that a single course of BEV contributed to improving KPS without marked adverse effects before surgery. Indeed, most patients with high-grade glioma received one course of BEV before surgery to alleviate peritumoral edema in two previous reports regarding BEV before surgery [4,5]. We performed operations for eight of the nine patients within the third week after BEV therapy and encountered no obvious complications after surgery. However, two previous reports documented high rates of complications to postoperative wound healing at 8% [13] and 35% [14] following preoperative BEV therapy in patients with recurrent glioblastoma. Abram et al. [15] recommended a strict 4-week interval between neoadjuvant BEV and surgery. In contrast, two reports documented no postoperative complications in patients with newly diagnosed glioblastoma who received surgery 21-27 days after BEV therapy [4,5]. Thus, the appropriate safety interval between neoadjuvant BEV initiation and surgery has remained controversial. Essentially, avoiding opportunistic risks such as diabetes mellitus and overuse of corticosteroids should be a minimum requirement. Operative findings in the BEV group, which included the ease of hemostasis and no effects on 5-ALA fluorescence, were consistent with the findings of a previous report [4]. Considering improvements in KPS and safety before, during, and after surgery, one-shot administration of BEV appears to hold promise as a neoadjuvant chemotherapy for glioblastoma.

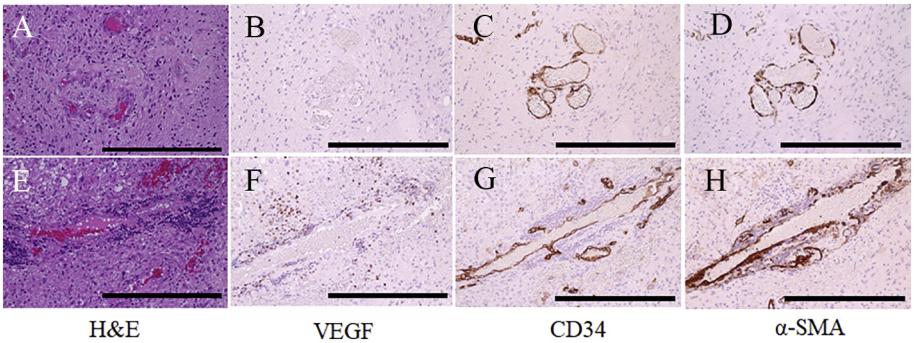

Figure 3. HE, VEGFA, CD34, and α-SMA on serial sections in case 4 of the BEV group (upper row) and case 12 in controls (lower row). VEGFA was entirely reduced on a section from the BEV group (B) but was detected in scattered cells in vessels and surrounding tumor cells (F). CD34 was detected in layer of vascular endothelium in both groups (C, G). The α-SMA was observed only in the layer of the vascular endothelium in a case from the BEV group (D) but was also detected in cells surrounding the vascular endothelium, suggesting vascular pericytes in a case from the control group (H). Bar = 250 μm.

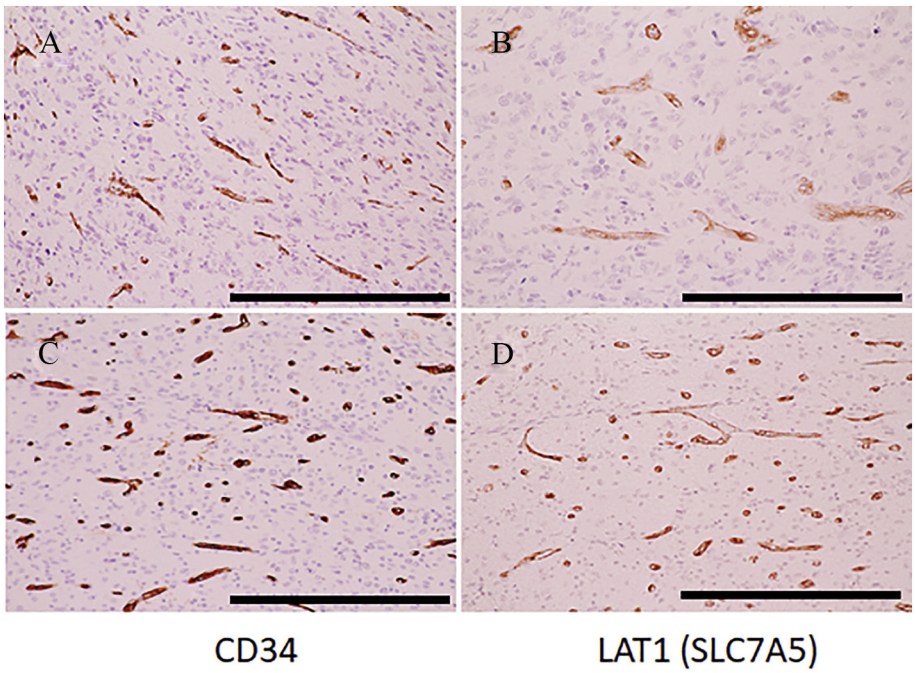

Figure 4. Illustrations of CD34 and LAT1 on serial sections from case 7 from the BEV group (upper row) and case 10 from the controls (lower row). Percentage of cells stained with LAT1 is lower in the BEV group than in controls. Bar = 250 μm.

Immunostaining showed that administration of even a single course of BEV led to significantly lower expression of VEGFA in glioblastomas. Inhibition of VEGFA expression would appear to be a compelling reason for the decrease in vascular density. This should be represented by attenuation of glomeruloid structures in the BEV group, as such structures are recognized to result from aggressive vascular proliferation. This study also showed ambiguous formation of pseudopalisading necrosis in the BEV group, although the reasons

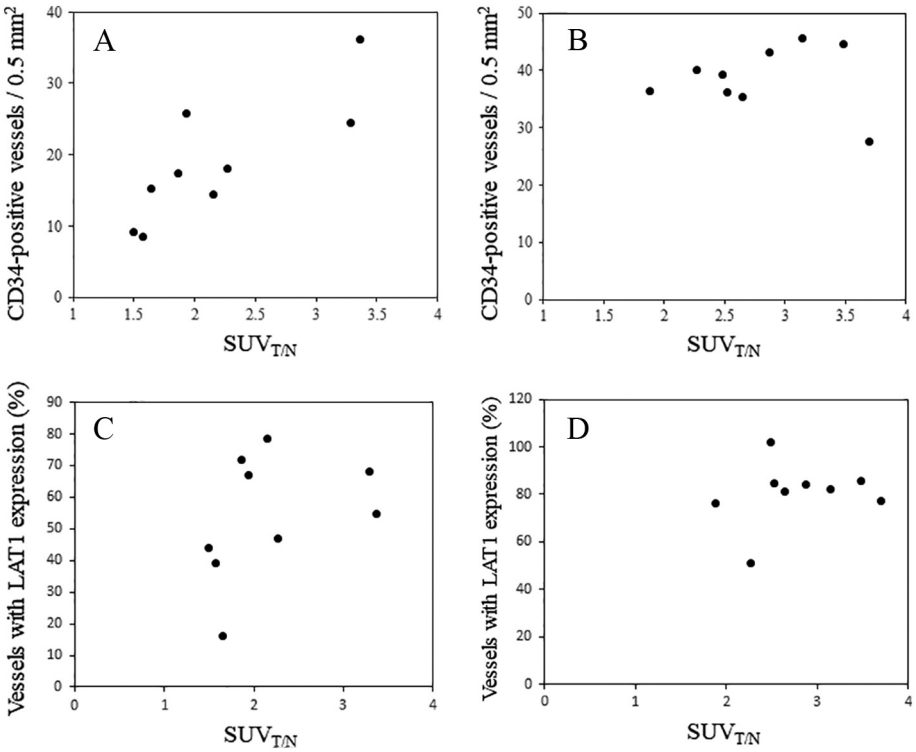

Figure 5. Assessments of correlations between $SUV_{T/N}$ and number of CD34-positive cells in the BEV group (A) and control group (B), and between $SUV_{T/N}$ and percentage of vessels accompanied with LAT1 expression in the BEV group (C) and control group (D). A significant correlation was only seen between $SUV_{T/N}$ and the number of CD34-positive cells in the BEV group (A).

for this change remain unclear. A previous study documented that five of six patients with glioblastoma who were preoperatively treated with BEV did not show clear pseudopalisading necrosis, and assumed that this finding had resulted from oxygenation in tumor tissues underlying vascular normalization due to BEV [4]. On the other hand, cell density and cell proliferation were relatively stable in the BEV group. These findings are supported by findings from previous reports [3–5]. In this study, the BEV group showed significantly fewer vessels surrounded by pericytes than the control group. This finding appears associated with the significant reduction in vascular density in the BEV group since proliferation of vascular pericytes is an essential mechanism of neovascularization in malignant glioma [6]. Since even a single administration of BEV leads to large histological changes in glioblastoma, sharing information on the use of BEV before surgery between physicians and pathologists is imperative.

In this study, ^{11}C-met-PET scans showed that even a single administration of BEV could lead to reduced accumulation of amino-acid tracer in tumor cells. In the literature, a clear trend toward changes in uptake of amino-acid tracers on PET at 1-2 months after starting BEV therapy has been reported, as a prompt decrease in the early phase for the first 2-4 weeks followed by a rebound in the late phase for weeks 4-8 [7,16,17]. A rapid reduction in the uptake of amino-acid tracers has been a subject of debate. First, this could be attributed to decreased permeability following restoration of the BBB under BEV therapy [17]. Another likely reason might be a decrease in microvascular density due to BEV because ^{11}C-met uptake depends on microvessel density and cell density within the glioma [18–20]. This hypothesis was supported by a finding of a significant correlation between $SUV_{T/N}$ and the number of CD34-positive vessels in the BEV group. The lack of correlation in the control group suggests that ^{11}C-met uptake largely depends on permeability in ordinary glioblastoma. Reduction of uptake induced by a cytocidal effect from BEV seems unlikely. Indeed, some studies, including our own, showed no significant decrease in tumor cell density and/or proliferation under BEV administration alone [4,5]. LAT1 could be involved as another mechanism for the reduction of ^{11}C-met uptake. Radiolabeled amino acid tracers after injection can enter glioma cells through the intact BBB *via* active diffusion, which is regulated by LAT1 [21,22]. Under conditions of restoration of the BBB due to BEV, LAT1 expression should largely influence the uptake of ^{11}C-met. A previous report documented that ^{11}C-met uptake depends on microvascular density combined with a high density or activity of LAT1 in endothelial cells in high-grade gliomas [22]. The percentage of LAT1-positive vessels was significantly lower in the BEV group than in controls, suggesting a reduction in LAT1 expression induced by BEV. However, no correlations between ^{11}C-met uptake and percentage of LAT1-positive vessels were identified in either group. This might have resulted from insufficient restoration of the BBB following a single administration of BEV and could be corroborated by the persistent enhancement in tumor on Gd-T1WI after BEV therapy (Figure 1).

Some limitations must be considered in this study. First, the sample size was small because few patients met all the inclusion criteria for the study. In particular, this limitation might have led to a finding of no significant difference in $SUV_{T/N}$ between before and after BEV therapy in the four patients who underwent consecutive PET. Rate of change in $SUV_{T/N}$ from before to after BEV was $-14.4\% \pm 6.0\%$ in this study, lower than the $-21.8\% \pm 13.9\%$ after two courses of BEV therapy previously reported [7]. Another reason for the lack of significant decrease in $SUV_{T/N}$ was that only a single course of BEV was insufficient to create an extreme reduction of ^{11}C-met uptake. On the other hand, this study with a small sample size involved possible selection bias for subjects. However, the similarities in terms of both the initial conditions (including tumor location and tumor size) and the outcomes seen in the two patient groups suggest that the degree of bias might have been small. As a second limitation, this study did not clarify the mechanisms underlying reductions in vascular pericytes after BEV therapy. Vascular pericytes are considered to be derived from glioma stem cells (GSC), actively remodeling of perivascular niches for GSC, and promoting therapeutic resistance [3,11,23]. Improvement of hypoxia in gliomas induced by normalization of tumor vessels due to BEV reportedly led to a reduced appearance of GSC [5]. A few microvessels with pericytes might result from the reduction of GSC led by oxygenation as an effect of BEV. As a third limitation, this study also did not explain the certain mechanisms for alleviation of LAT1 expression under BEV therapy. One study showed a relationship between LAT1 expression and VEGF in non–small cell lung cancer [24]. Another study showed that expressing LAT1 has been considered to require hypoxic conditions within the tumor [25]. A possible reason for the reduction in LAT1 expression might be improvement of the hypoxic condition within the tumor due to BEV, which was likewise a reason for the reduction of vascular pericytes.

Funding

This study was supported in part by a Grant-in-Aid for JSPS KAKENHI (grant no. 17K11590) and a Strategic Medical Science Research (grant no. S1491001) from the Ministry of Education, Culture, Sports, Science and Technology of Japan.

Conflict of Interest

The authors declare that they have no conflict of interest.

Compliance with Ethical Standards

All study protocols were approved by the ethics committee at our institute (No. H22-96). All procedures performed in studies involving human participants were conducted in accordance with the ethical standards of the institutional and/or national research committee and with the 1964 Declaration of Helsinki and its later amendments or comparable ethical standards.

Informed Consent

Informed consent was obtained from all individual participants included in the study.

References

[1] Gilbert MR, Dignam JJ, Armstrong TS, Wefel JS, Blumenthal DT and Vogelbaum MA, et al (2014). A randomized trial of bevacizumab for newly diagnosed glioblastoma. *New Eng J Med* **370**(8), 699–708. https://doi.org/10.1056/NEJMoa1308573.

[2] Jain RK (2001). Normalizing tumor vasculature with anti-angiogenic therapy: a new paradigm for combination therapy. *Nat Med* **7**(9), 987–989. https://doi.org/10.1038/nm0901-987nm0901-987. pii.

[3] Okamoto S, Nitta M, Maruyama T, Sawada T, Komori T and Okada Y, et al (2016). Bevacizumab changes vascular structure and modulates the expression of angiogenic factors in recurrent malignant gliomas. *Brain Tumor Pathol* **33**(2), 129–136. https://doi.org/10.1007/s10014-016-0248-6.

[4] Tamura R, Tanaka T, Miyake K, Tabei Y, Ohara K and Sampetrean O, et al (2016). Histopathological investigation of glioblastomas resected under bevacizumab treatment. *Oncotarget* **7**(32), 52423–52435. https://doi.org/10.18632/oncotarget.9387.

[5] Yamamoto Y, Tamura R, Tanaka T, Ohara K, Tokuda Y and Miyake K (2017). et al. "Paradoxical" findings of tumor vascularity and oxygenation in recurrent glioblastomas refractory to bevacizumab. *Oncotarget* **8**(61), 103890−103899. https://doi.org/10.18632/oncotarget.21978.

[6] Sun H, Guo D, Su Y, Yu D, Wang Q and Wang T, et al (2014). Hyperplasia of pericytes is one of the main characteristics of microvascular architecture in malignant glioma. *PloS one* **9**(12):e114246. https://doi.org/10.1371/journal.-pone.0114246.

[7] Beppu T, Terasaki K, Sasaki T, Sato Y, Tomabechi M and Kato K, et al (2016). MRI and 11C-methyl-L-methionine PET differentiate bevacizumab true responders after initiating therapy for recurrent glioblastoma. *Clin Nucl Med* **41**(11), 852−857. https://doi.org/10.1097/RLU.0000000000001377.

[8] Pascali CBA, Iwata R, Decise D, Crippa F and Bombardieri E (1999). High efficiency preparation of [11C]methionine by on-column [11C]methylation on C18 Sep-Pak. *J Labelled Comp Radiopharm* **42**, 715−724.

[9] Ellingson BM, Wen PY and Cloughesy TF (2017). Modified criteria for radiographic response assessment in glioblastoma clinical trials. *Neurotherapeutics* **14**(2), 307−320. https://doi.org/10.1007/s13311-016-0507-6.

[10] Wen PY, Macdonald DR, Reardon DA, Cloughesy TF, Sorensen AG and Galanis E, et al (2010). Updated response assessment criteria for high-grade gliomas: response assessment in neuro-oncology working group. *J Clin Oncol* **28**(11). https://doi.org/10.1200/JCO.2009.26.3541.

[11] Shepro D and Morel NM (1993). Pericyte physiology. *FASEB J* **7**(11), 1031−1038.

[12] Li J, Wang M, Won M, Shaw EG, Coughlin C and Curran Jr WJ, et al (2011). Validation and simplification of the Radiation Therapy Oncology Group recursive partitioning analysis classification for glioblastoma. *Int J Radiat Oncol Biol Phys* **81**(3), 623−630. https://doi.org/10.1016/j.ij-robp.2010.06.012.

[13] Chamberlain MC and Johnston SK (2010). Salvage therapy with single agent bevacizumab for recurrent glioblastoma. *J Neurooncol* **96**(2), 259−269. https://doi.org/10.1007/s11060-009-9957-6.

[14] Clark AJ, Butowski NA, Chang SM, Prados MD, Clarke J and Polley MY, et al (2011). Impact of bevacizumab chemotherapy on craniotomy wound healing. *J Neurosurg* **114**(6), 1609−1616. https://doi.org/10.3171/2010.10.JNS101042.

[15] Abrams DA, Hanson JA, Brown JM, Hsu FP, Delashaw Jr JB and Bota DA (2015). Timing of surgery and bevacizumab therapy in neurosurgical patients with recurrent high grade glioma. *J Clin Neurosci* **22**(1), 35−39. https://doi.org/10.1016/j.jocn.2014.05.054.

[16] Harris RJ, Cloughesy TF, Pope WB, Nghiemphu PL, Lai A and Zaw T, et al (2012). 18F-FDOPA and 18F-FLT positron emission tomography parametric response maps predict response in recurrent malignant gliomas treated with bevacizumab. *Neuro-Oncol* **14**(8), 1079−1089. https://doi.org/10.1093/neuonc/nos141.

[17] Schwarzenberg J, Czernin J, Cloughesy TF, Ellingson BM, Pope WB, Geist C et al. 3′-Deoxy-3'-18F-fluorothymidine PET and MRI for early survival predictions in patients with recurrent malignant glioma treated with bevacizumab. J Nucl Med. 2012;53(1):29−36. doi:jnumed.111.092387 [pii]https://doi.org/10.2967/jnumed.111.092387.

[18] Di Ieva A, Grizzi F, Tschabitscher M, Colombo P, Casali M and Simonelli M, et al (2010). Correlation of microvascular fractal dimension with positron emission tomography [(11)C]-methionine uptake in glioblastoma multiforme: preliminary findings. *Microvasc Res* **80**(2), 267−273. https://doi.org/10.1016/j.mvr.2010.04.003.

[19] Okita Y, Kinoshita M, Goto T, Kagawa N, Kishima H and Shimosegawa E, et al (2010). (11)C-methionine uptake correlates with tumor cell density rather than with microvessel density in glioma: a stereotactic image-histology comparison. *Neuroimage* **49**(4), 2977−2982. https://doi.org/10.1016/j.neu-roimage.2009.11.024.

[20] Beppu T, Sato Y, Sasaki T, Terasaki K, Yamashita F and Sasaki M, et al (2019). Comparisons between PET with 11C-methyl-L-methionine and arterial spin labeling perfusion imaging in recurrent glioblastomas treated with bevacizumab. *Clin Nucl Med* **44**(3), 186−193. https://doi.org/10.1097/RLU.0000000000002417.

[21] Langen KJ, Galldiks N, Hattingen E and Shah NJ (2017). Advances in neuro-oncology imaging. *Nat Rev Neurol* **13**(5), 279−289. https://doi.org/10.1038/nrneurol.2017.44.

[22] Okubo S, Zhen HN, Kawai N, Nishiyama Y, Haba R and Tamiya T (2010). Correlation of L-methyl-11C-methionine (MET) uptake with L-type amino acid transporter 1 in human gliomas. *J Neurooncol* **99**(2), 217−225. https://doi.org/10.1007/s11060-010-0117-9.

[23] Cheng L, Huang Z, Zhou W, Wu Q, Donnola S and Liu JK, et al (2013). Glioblastoma stem cells generate vascular pericytes to support vessel function and tumor growth. *Cell* **153**(1), 139−152. https://doi.org/10.1016/j.cell.2013.02.021.

[24] Kaira K, Oriuchi N, Shimizu K, Ishikita T, Higuchi T and Imai H, et al (2009). Correlation of angiogenesis with 18F-FMT and 18F-FDG uptake in non−small cell lung cancer. *Cancer Sci* **100**(4), 753−758. https://doi.org/10.1111/j.1349-7006.2008.01077.x.

[25] Kaira K, Oriuchi N, Takahashi T, Nakagawa K, Ohde Y and Okumura T, et al (2011). LAT1 expression is closely associated with hypoxic markers and mTOR in resected non−small cell lung cancer. *Am J Transl Res* **3**(5), 468−478.